Please cite the Published Version

Bernalte, Elena , Crapnell, Robert D. , Oliveira, Anna C.M., Fougerol, Milo, Augusto, Karen K. L. , Khan, Muhzamil A , Wurzer, Christian, Masek, Ondrej, Singla, Pankaj, Peeters, Marloes, Jayakumar, Anjali, Munoz, Rodrigo A. A. , and Banks, Craig E (2025) Biochar doped recycled PLA for carbendazim detection in environmental water using additive manufactured electrodes. Materials Today Communications, 47. 113287

DOI: https://doi.org/10.1016/j.mtcomm.2025.113287

Publisher: Elsevier

Version: Published Version

Downloaded from: https://e-space.mmu.ac.uk/641968/

Usage rights: Creative Commons: Attribution 4.0

Additional Information: This is an open access article published in Materials Today Communi-

cations, by Elsevier.

Data Access Statement: Data will be made available on request.

Enquiries:

If you have questions about this document, contact openresearch@mmu.ac.uk. Please include the URL of the record in e-space. If you believe that your, or a third party's rights have been compromised through this document please see our Take Down policy (available from https://www.mmu.ac.uk/library/using-the-library/policies-and-guidelines)

ELSEVIER

Contents lists available at ScienceDirect

Materials Today Communications

journal homepage: www.elsevier.com/locate/mtcomm





Biochar doped recycled PLA for carbendazim detection in environmental water using additive manufactured electrodes

Elena Bernalte ^{a,1}, Robert D. Crapnell ^{a,1}, Ana C.M. Oliveira ^{a,c}, Milo Fougerol ^{a,b}, Karen K.L. Augusto ^{a,c}, Muhzamil Khan ^a, Christian Wurzer ^d, Ondrej Masek ^d, Pankaj Singla ^e, Marloes Peeters ^e, Anjali Jayakumar ^f, Rodrigo A.A. Muñoz ^c, Craig E. Banks ^{a,*}

- ^a Faculty of Science and Engineering, Manchester Metropolitan University, Dalton Building, Chester Street, M1 5GD, United Kingdom
- b Department of Physical Measurements, Sorbonne Paris North University, Place du 8 Mai 1945, Saint-Denis 93200, France
- ^c Institute of Chemistry. Federal University of Uberlândia, Uberlândia, Minas Gerais 38400-902, Brazil
- ^d UK Biochar Research Centre, School of GeoSciences, University of Edinburgh, Edinburgh, EH9 3FF, United Kingdom
- e Department of Chemical Engineering, Nancy Rothwell Building, East Booth Street, The University of Manchester, Manchester M13 9QS, United Kingdom
- f School of Engineering, Newcastle University, Newcastle Upon Tyne NE17RU, United Kingdom

ARTICLE INFO

Keywords: Additive manufacturing 3D-printing Biochar Sustainability Electrochemistry Circular economy PLA

ABSTRACT

Additive manufacturing electrochemistry offers transformative potential for developing bespoke, low-cost electrodes for electroanalytical applications. However, ensuring sustainability in this rapidly expanding field is essential, requiring alignment with green chemistry principles, the circular economy, and the United Nations Sustainable Development Goals (SDGs). This study addresses this challenge by developing the first biochar-based conductive additive manufacturing feedstock, combining recycled PLA, bio-based castor oil, carbon black, and softwood-based biochar (SWP10). Filaments with varying SWP10 content (1-40 %) were produced, with up to 20 wt% SWP10 (SWP10-20) maintaining good printability. Electrochemical characterisation identified SWP10-2.5 (2.5 wt%) as the optimal composition, achieving improved electrochemical performance while enhancing sustainability. Both SWP10-2.5 and SWP10-20 were tested for electroanalytical applications, demonstrating their effectiveness in detecting carbendazim, an important environmental contaminant. The electrodes exhibited low limits of detection (57 nM for SWP10-2.5 and 78 nM for SWP10-20) and wide linear ranges (0.2-40 µM), outperforming several previously reported sensors. Furthermore, both electrodes were successfully applied for the detection of carbendazim in spiked real river and lake water samples, achieving recoveries between 92.5 % and 107.2 %. These results demonstrate that by optimising biochar and carbon black ratios, it is possible to enhance the sustainability of conductive additive manufacturing materials without compromising electrochemical or electroanalytical performance. This work highlights a pathway toward more environmentally friendly electroanalytical platforms, supporting the SDGs while addressing real-world challenges in environmental monitoring and sensor development.

1. Introduction

The Sustainable Development Goals (SDGs) published by the United Nations (UN) are a crucial, comprehensive framework designed to be the blueprint for peace and prosperity for people and the planet [1]. They take a holistic approach to tackling the world's most pressing challenges, including poverty, inequality, climate change, environmental degradation, peace, and justice. The SDGs apply to all countries, aiming

to foster global cooperation, and encouraging innovation to produce balanced and integrated approaches to sustainable development. Many of the SDGs primarily aim to protect the planet by focussing on sustainable practices and conserving natural resources. This includes Goal 12 entitled "Responsible Consumption and Production", which aims to achieve the sustainable management and efficient use of natural resources by 2030 by reducing the amount used and minimising waste throughout production processes [2].

E-mail address: c.banks@mmu.ac.uk (C.E. Banks).

^{*} Corresponding author.

 $^{^{1}\,}$ These authors contributed equally.

One manufacturing methodology that has received significant attention due to its strong synergy with Goal 12 of the SDGs is additive manufacturing (AM) [3,4] due to its significant material and energy efficiency, on-demand production, recycling capabilities, and localised production. AM encompasses 7 unique manufacturing processes that all create 3-dimensional objects in a layer-by-layer pattern. Of the available techniques, Fused Filament Fabrication (FFF, also known as Fused Deposition Modelling or FDM) is one of the most utilised globally due to its low-cost of entry, small machine size, and commercially available low-cost materials, making it popular with industry, academia, and home enthusiasts alike. FFF functions through the deposition of thin, micrometre lines of thermoplastic material, using these to build up the final 3-dimensional object. Improvements in the sustainability of FFF have come through various avenues such as enhancing the energy efficiency of machines, optimising print parameters to increase material efficiency, transitioning toward recycled materials [5,6], and developing printable bio-based materials [7,8].

One area of research that has seen a rapid increase in the number of publications utilising FFF is additive manufacturing electrochemistry, due to the excellent sensing capabilities and low cost of electrochemistry [9-11], where it has been used to make electrochemical cells, accessories [12], equipment [13], and electrodes [14]. For the last purpose, commercially available conductive filament was initially explored, with researchers concentrating efforts in optimising the printing parameters [15–18], post-print treatment [19–21], and electrode designs [22]. Even so, the electrochemical performance of these systems was hindered by the poor conductivity of the material. As such, researchers have begun producing their own bespoke filament with enhanced electrochemical properties [23], improved chemical resistances and stabilities [24–27], as well as improved sustainability [28,29]. In this regard, Sigley et al. [30] were the first to report the use of recycled plastic in their conductive filament production. They utilised recycled poly(lactic acid) (rPLA) derived from disposable coffee pods to produce filament, finally using this to detect caffeine within tea and coffee samples and coining the term circular economy electrochemistry. Further work has been developed by research team who have reporting the first additive manufacturing filament embedded with gold nanoparticles using rPLA [31] and also the first production of the a conductive filament comprise of poly(propylene and carbon black. [32] Various avenues have been explored to improve the sustainability of the conductive filament researchers are producing, such as changing from synthetic plasticisers to natural bio-based alternatives [33-35], and replacing parts of the petrochemical derived carbon sources with naturally occurring ones [36,37]. In this regard, biochar becomes an intriguing possibility.

Biochar is a carbon-rich material produced through the pyrolysis of biomass in an oxygen-limited environment. This process involves heating organic materials, such as agricultural waste, at high temperatures, resulting in a stable, porous structure with a high surface area [38]. Biochar's unique properties, including its excellent electrical conductivity, chemical stability, and tuneable surface functional groups, make it an attractive material for electrochemical applications [39]. In electrochemistry, biochar is used as an electrode material in supercapacitors [40,41], batteries [42–44], and hydrogen storage devices [45,46]. As such, the replacement of petrochemically derived carbon sources with biochar has the potential to greatly improve the sustainability of conductive additive manufacturing feedstock [47].

In this work, we therefore look to produce the first biochar-based conductive additive manufacturing feedstock by combining recycled PLA, bio-based castor oil, and softwood-based biochar [48]. Through optimising the ratio of carbon black and biochar we can elucidate ways to further improve the sustainability of conductive additive manufacturing feedstock, without compromising the electrochemical performance. Once developed, this first biochar-based conductive filament was applied to the detection of carbendazim, a broad-spectrum fungicide that is regulated in many countries [49]. Carbendazim is regulated in many countries to ensure that the potential health risks of

high doses are not realised such as kidney and liver damage and endocrine disruption [50,51]. This highlights how high-performance additive manufacturing filament can be produced to meet real electroanalytical challenges, whilst improving the sustainability of the field.

2. Experimental section

2.1. Chemicals

All chemicals used throughout this work were used as received without any further purification. All aqueous solutions were prepared with deionised water of a measured resistivity not <18.2 M Ω cm, sourced from a Milli-Q Integral 3 system from Millipore UK (Watford, UK). Hexaammineruthenium (III) chloride (RuHex, 98 %), castor oil, potassium ferricyanide (99 %), potassium ferrocyanide (98.5-102 %), sodium hydroxide (>98 %), potassium chloride (99.0–100.5 %), acetic acid (>99 %), boric acid (99 + %), and phosphoric acid (extra pure, 85 %) were purchased from Merck (Gillingham, UK). Carbendazim (>98 %) was purchased from Tokyo Chemical Industries (Zwijndrecht, Belgium), Carbon black was purchased from PI-KEM (Tamworth, UK). Recycled poly(lactic acid) (rPLA) was purchased from Gianeco (Turin, Italy). River water samples were obtained in accordance with EPA guidelines from the River Irwell, Greater Manchester, UK (approx. location: 53.517464, -2.302739). Lake water samples were collected from Llyn Llydaw, Wales, UK (approx. location: 53.073056, -4.040694).

2.2. Production of biochar SWP and SWP10

Production of the biochars is described in detail in Wurzer & Masek (2021) [48]. Briefly, commercial softwood pellets (SWP) were used as a biomass precursor for both biochars, while 10 % (wt. d.b.) of ochre, a Fe-rich mining waste material, was added to the biomass before pyrolysis for SWP10. The precursors were then heated to 550 °C in $\rm N_2$ atmosphere, held for 45 min, before cooling down to room temperature. A subsequent activation step at 800 °C under CO $_{\rm 2}$ atmosphere was conducted to increase the surface area of the biochar samples.

2.3. Recycled filament production

Recycled poly(lactic acid) (rPLA) has been dried according to our previous work. [31] The polymer compositions were prepared through the addition of appropriate amounts of rPLA (60 wt%), castor oil (10 wt %), and carbon filler (30 wt%) in a chamber of 63 cm³. The overall 30 wt % of carbon filler was comprised of different amounts of carbon black and biochar (SWP and SWP10). All filaments made throughout this work utilised 10 wt% castor oil as a plasticiser [33]. This is processed as reported to our previous work [31] where the compounds are mixed using a Thermo Haake Polydrive dynameter equipped with a Thermo Haake Rheomix 600 mixer (Thermo-Haake, Germany), operating at 190 °C with Banbury rotors at 70 rpm for 5 min. After mixing, the resulting polymer composites were cooled to room temperature and subsequently granulated using a Rapid Granulator 1528 (Rapid, Sweden) to reduce the particle size. The granulated composites were then fed into the hopper of a Filabot EX2 extrusion line (Filabot, VA, United States), which was configured with a single screw and a heat zone set to 190 $^{\circ}\text{C}.$ The molten polymer was extruded through a 1.75 mm die head, passed along an Airpath cooling line (Filabot, VA, United States), and wound onto a spool. The resulting filament was then ready for use in additive manufacturing.

2.4. Additive manufacturing of the electrodes

All computer designs and 3MF files in this manuscript were produced using Fusion 360® (Autodesk®, CA, United States). These files were sliced and converted to GCODE files in PrusaSlicer (Prusa Research,

Prague, Czech Republic). The additive manufactured electrodes were produced using FFF technology on a Prusa i3 MK3S+ (Prusa Research, Prague, Czech Republic). All additive manufactured electrodes were printed using identical printer components and printing parameters, namely a 0.6 mm nozzle with a nozzle temperature of 215 °C, 100 % rectilinear infill [15], 0.15 mm layer height, and print speed of 35 mm s $^{-1}$. Electrodes were printed on a smoothed PEI steel sheet heated to 50 °C without the need of supportive tape or glue.

2.5. Physicochemical characterisation

X-ray Photoelectron Spectroscopy (XPS) data were acquired using an AXIS Supra (Kratos, UK), equipped with a monochromatic Al X-ray source (1486.6 eV) operating at 225 W and a hemispherical sector analyser. It was operated in fixed transmission mode with a pass energy of 160 eV for survey scans and 20 eV for region scans with the collimator operating in slot mode for an analysis area of approximately 700×300 μm , the FWHM of the Ag 3d5/2 peak using a pass energy of 20 eV was 0.613 eV. The binding energy scale was calibrated by setting the graphitic sp 2 C 1 s peak to 284.5 eV; this calibration is acknowledged to be flawed [52] but was nonetheless used in the absence of reasonable alternatives, and because only limited information was to be inferred from absolute peak positions.

Scanning Electron Microscopy (SEM) micrographs were obtained using a Crossbeam 350 Focussed Ion Beam – Scanning Electron Microscope (FIB-SEM) (Carl Zeiss Ltd., Cambridge, UK) fitted with a field emission electron gun. Secondary electron imaging was completed using a Secondary Electron Secondary Ion (SESI) detector. Samples were mounted on the aluminium SEM pin stubs (12 mm diameter, Agar Scientific, Essex, UK) using adhesive carbon tabs (12 mm diameter, Agar Scientific, Essex, UK) and coated with a 5 nm layer of Au/Pd metal using a Leica EM ACE200 coating system before imaging.

Raman spectroscopy was performed on a DXR Raman Microscope (Thermo Scientific Inc., Waltham, MA, USA) configured with a 532 nm laser and operates using OMNIC 9 software.

2.6. Electrochemical experiments

All electrochemical experiments were performed on an Autolab 100 N potentiostat controlled by NOVA 2.1.7 (Utrecht, The Netherlands). Identical additive manufactured electrodes were used throughout this work for all filaments, printed in a lollipop shape (Ø 5 mm disc with a connection stem of 8 mm connection length, 2 mm width and 1 mm thickness [22]) alongside an external commercial Ag| AgCl/KCl (3 M) reference electrode with a nichrome wire counter electrode. All solutions of [Ru(NH₃)₆]³⁺ were purged of O₂ thoroughly using N₂ prior to any electrochemical experiments. Solutions of [Fe (CN)₆]^{4-/3-} were prepared in the same way without the need of further degassing.

Electrochemical impedance spectroscopy (EIS) was recorded in the frequency range 0.1 Hz to 100 kHz applying 10 mV of signal amplitude to perturb the system under quiescent conditions. NOVA 2.1.7 software was used to fit Nyquist plots obtained to adequate equivalent circuit.

Activation of the additive manufactured electrodes was performed, where applicable, electrochemically in NaOH (0.5 M), as described in the literature [53]. Briefly, the additive manufactured electrodes were connected as the working electrode in conjunction with a nichrome wire coil counter and Ag|AgCl/KCl (3 M) reference electrode and placed in a solution of 0.5 M NaOH. Chronoamperometry was used to activate the additive manufactured electrodes by applying a set voltage of \pm 1.4 V for 200 s, followed by applying \pm 1.0 V for 200 s. The additive manufactured electrodes were then thoroughly rinsed with deionised water and dried under compressed air before further use.

Spiked real water samples were analysed through the standard addition method, where the river or lake water was spiked with 25 μ M of carbendazim and diluted in BR buffer (pH = 4, 1:10). Analysis was

performed using differential pulse voltammetry with the following parameters: start potential =+0.6 V; stop potential =+1.2 V; step potential =0.05 V; modulation amplitude =0.08 V; modulation time =0.07 s; interval time =0.2 s. Recovery values were calculated using the standard addition method, whereby the obtained intercept value was divided by the slope of the curve, taking into account the dilution of the sample.

All electrochemical measurements in this work were performed in triplicate with three separate electrodes.

3. Results and discussion

The replacement of petrochemically derived carbon sources within conductive additive manufacturing feedstock has the potential to further improve the sustainability of filament production and additive manufacturing electrochemistry as a field. Biochar, a carbon source derived from the pyrolysis of biomass, has been identified as a potential contributor to this end and as such we explore its incorporation into conductive filament for the first time using recycled PLA as the base polymer and castor oil as a bio-based plasticiser [33].

3.1. Production and characterisation of biochar integrated filament

To investigate the effect of biochar incorporation on the performance of conductive additive manufacturing filament, well characterised biochar found within the literature made from softwood pellets (SWP) and SWP with 10 % ochre (SWP10) was used [48,54]. A schematic of filament production is shown in Fig. 1A, whereby the materials were all added into the chamber of a heated rheomixer and mixed for 5 min with Banbury rotors at 190 $^{\circ}$ C. Utilisation of thermal mixing over other methods such as solvent mixing is preferential due to the reduced production time, removal of toxic solvents, and ability to power the machinery through only green energy [23].

For the production of all filaments, the amount of recycled PLA (60 wt%) and castor oil (10 wt%) was kept constant, along with the total amount of carbon filler (30 wt%). All filaments were compared to a benchmark, where the whole 30 wt% of filler was commercially purchased carbon black (CB). The amount of both forms of biochar, SWP and SWP10, that could replace CB was investigated by progressively increasing the amount of CB replaced with biochar. For SWP 10 % of the overall CB content was able to be replaced, whereas for the SWP10 up to 40 % of the CB content was able to be replaced whilst still producing a filament. This was attributed primarily to the smaller particle morphology of SWP-10, which allowed for easier incorporation. The filaments investigated are referred to by the amount of CB replaced with biochar, with SWP10-2.5 indicating 2.5 % of CB has been replaced. Due to the larger incorporation of SWP10 possible, this was chosen for further studies. Fig. 1B shows photographs of filaments produced replacing 0 % of the CB, 20 % of the CB, and 40 % of the CB, with filaments produced replacing 1, 2.5, 5 and 10 % shown in Figure S1. It can be seen how the low-temperature flexibility of the filaments overall deteriorates upon the inclusion of increased amounts of biochar. This had a significant impact on the printability of the filaments, with no reliable printing achievable with filaments replacing more that 20 % of the CB with biochar. The bulk resistance of the biochar doped filaments was next investigated, where SWP10-2.5 was found to produce a value of $28 \pm 2 \,\Omega\,\text{cm}^{-1}$, which was an improvement when compared to the 34 \pm 4 Ω cm^{-1} for SWP10–0. When increasing the biochar content up to SWP10-20, there was no significant increase in the bulk resistance compared to SWP10–0, with a value of 35 \pm 2 Ω cm^{-1} measured. For SWP10–40 there was a large increase in the bulk resistance up to 84 $\pm\,6$ Ω cm⁻¹, so combined with the poor printability, it was decided to no longer explore this filament.

Fig. 1 C shows photographs of the electrodes printed from SWP10-0, SWP10-2.5, and SWP10-2.0, with the electrodes printed from SWP10-1, SWP10-5, and SWP10-10 shown in Figure S2, where in all cases

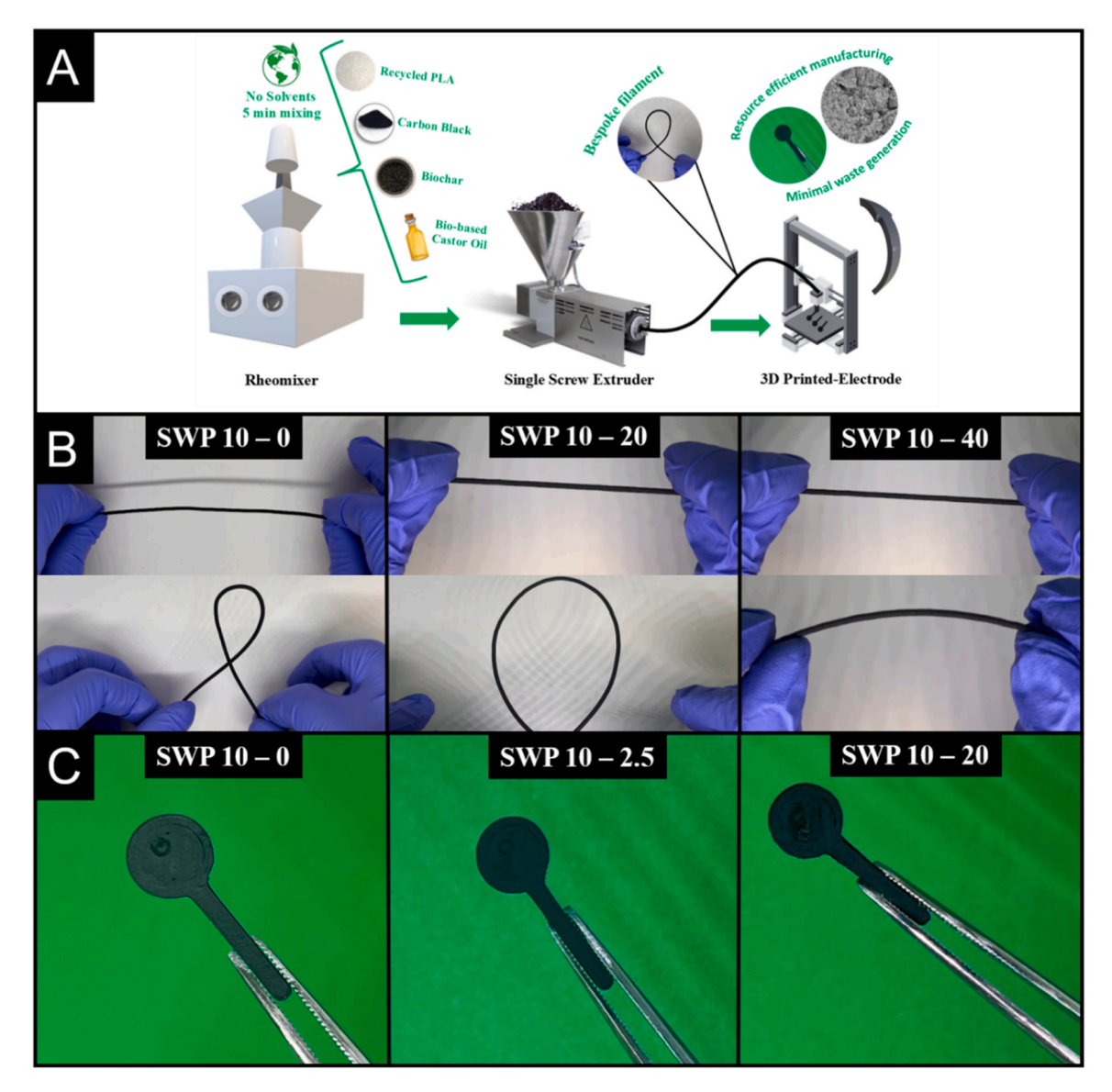


Fig. 1. A) Filament production scheme, B) Photographs highlighting the low temperature flexibility of the 0, 20 and 40 wt% CB/PLA/SWP10 filaments, and C) Photographs of electrodes with varying percentages of biochar.

excellent quality electrodes were produced. As the SWP10–2.5 filament showed the best conductivity, and the SWP10–20 showed the largest replacement of CB with biochar, these two filaments were chosen to study further, along with SWP10–0 as a benchmark.

3.2. Physicochemical characterisation of biochar integrated filament

The successfully printed electrodes were then physicochemically characterised to elucidate the nature of their surfaces prior to electrochemical studies. It is commonplace within the literature to perform a post-print activation step on the electrodes to improve their electrochemical performance. It is important to note that this step is not necessary to get the electrodes to work, it simply improves their performance. Bespoke as-printed electrodes can already outperform commercial activated ones, as reported previously [30]. In this work, the electrodes were activated using chronoamperometry in 0.5 M NaOH, which is the most commonly utilised method in the literature [20,53, 55]. The electrodes before and after activation were then studied using X-ray photoelectron spectroscopy (XPS), Raman spectroscopy, and scanning electron microscopy (SEM).

Fig. 2A-C shows the XPS wide survey scan, C1 s scan, and O1 s scan

for the activated SWP10-20 electrode, with the equivalent plots for SWP10-20 before activation, and SWP10-0 before and after activation included in Figure S3 and S4, respectively. In all cases, in the survey scans, there are large intensity peaks found at ~285 eV, corresponding to the C 1 s region, and at \sim 535 eV, corresponding to the O 1 s region. In some cases, small intensity peaks can be observed for Si, N, and Na, which are known to be common contaminants within the plastic or carbon sources or used within the activation procedure. Interestingly, there was no peak observed for Fe, even though the ochre added to the biochar is known to be Fe rich [48]. This is attributed to the low amount of Fe within the biochar and in turn, low amount of biochar when considering the composition of the whole filament. When fitting the C 1 s regions, in all cases four symmetric peaks were used corresponding to the sp³ hybridised carbon environments, C-C/C-H, C-O, C=O, and O-C=O. For only PLA, three peaks of similar intensity for the C-C/C-H, C=O, and O-C=O would be expected, indicating the additional presence of the bio-based plasticiser castor oil or carbon black on the surface of the electrodes. In addition to these symmetric peaks, one asymmetric peak was required at ~284.5 eV, attributed to the X-ray photoelectron emission of sp² graphitic carbon [56,57]. For both SWP10-0 and SWP10-20, a similar trend is observed whereby a large increase in the

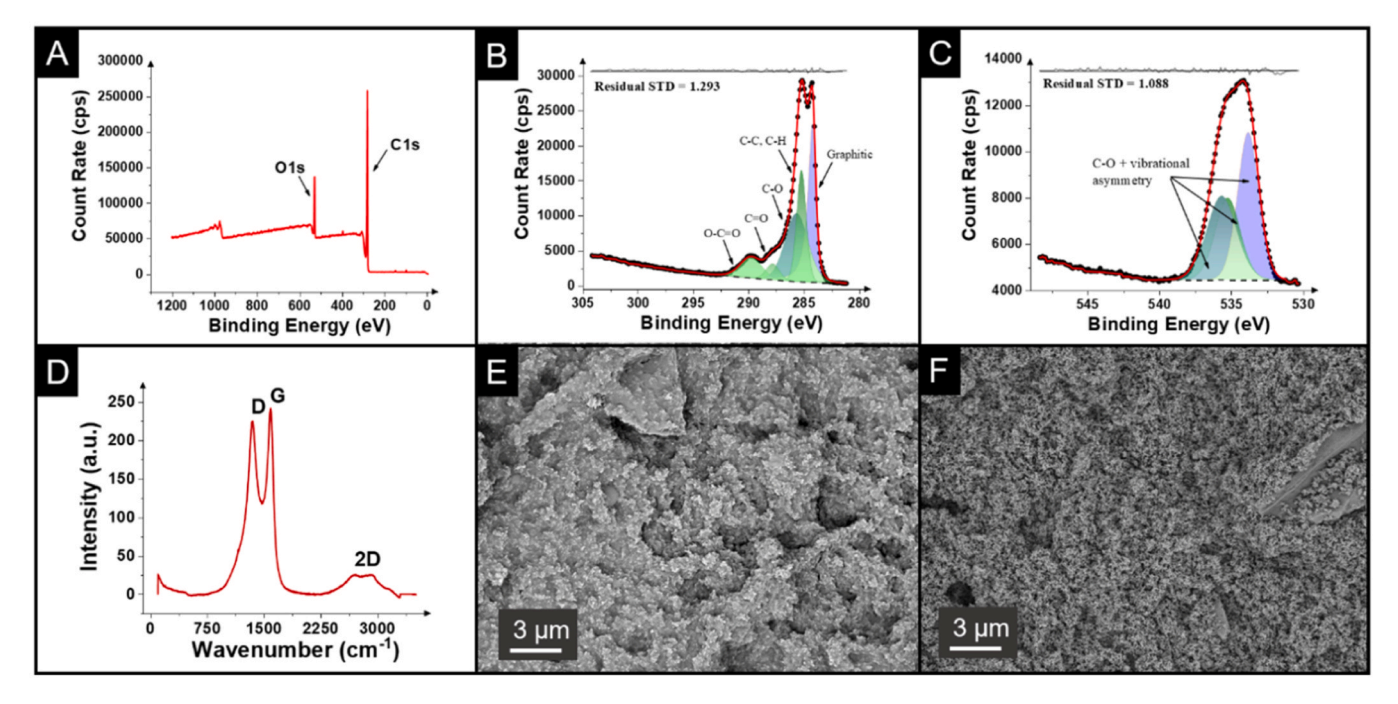


Fig. 2. XPS data of the SPW10–20 electrodes after electrochemical activation: A) Survey scan B) C 1 s scan and C) O 1 s scan. D) Raman spectra for the SPW10–20 electrodes. SEM images of the SPW10–20 electrodes E) before and F) after electrochemical activation.

atomic concentration of the sp³ graphitic carbon is seen after electrochemical activation. For SWP-0 this increases from 10 % before activation to 35 % after activation, with it increasing from 18 % in SWP-20–31 % after activation. This indicates the removal of non-conductive surface material, revealing increased amounts of the graphitic carbon beneath, either within the biochar or carbon black. Interestingly, the C-O atomic concentration is significantly higher in the SWP10–20 (31 %) than in the SWP10–0 sample (8 %) which can be attributed to the surface functionalities of the SWP10 biochar, and its increased size which can lead to increased amounts of protrusion from the printed surface.

The printed electrodes were then examined through Raman spectroscopy, with the SWP10-20 shown in Fig. 2D and the SWP10-0 shown in Figure S5. In both samples, there are three clearly defined peaks present at 1338, 1572, and 2680 cm⁻¹, which are attributed to the characteristic D-, G-, and 2D bands for graphitic-like structures. Through calculating the I_D/I_G ratio for the samples of 0.93 for SWP10-20 and 0.92 for SWP10-0 we can see that in both cases the value falls around approximately 1, indicating disorder in the graphitic structures, which is expected with carbon black and confirms its presence on the surface. These findings were further investigated with SEM, presented for SWP10-20 before activation in Fig. 2E and after activation in Fig. 2F. Increased magnification images can be seen in Figure S6. The corresponding images for SWP10-0 can be seen in Figure S7. In both cases, before activation, there is the clear presence of a thin layer of polymeric material under which are the morphologies expected for the CB structures. In the SWP10-20, larger morphologies can also be seen attributed to the biochar. Once activated, in both cases the polymeric layer is removed from the surface leaving clear images of the CB particles and in the case of SWP10-20 the larger flake structures of the biochar. This shows agreement with the XPS data above indicating the revealing of increased amounts of sp² hybridised carbon.

3.3. Electrochemical characterisation of biochar filament

After physicochemical characterisation, the electrodes were tested electrochemically against both outer and inner sphere redox probes. Initially, scan rate studies were performed for all electrodes against the near-ideal outer sphere redox probe hexaamineruthenium (III) chloride ([Ru(NH₃)₆]³⁺) as this allowed for the best determination of the heterogeneous electron (charge) transfer rate constant (k^0) and real electrochemical area (A_e) [58,59]. Importantly, the kinetics of this outer sphere probe are minimally affected by the electrode surface chemistry [60,61]. Figs. 3A and 3B show the cyclic voltammograms (CVs, $\nu=5-500~\text{mV}~\text{s}^{-1}$) obtained for SWP10–0 and SWP10–20, respectively, with the results for SWP10–1, SWP10–2.5, SWP10–5 and SWP10–10 shown in Figure S8.

It can be seen that in each case, the expected one electron process was observed, with the associated inset Randles-Ševčík plots confirming the diffusion-controlled nature of the redox processes [60]. The key electrochemical parameters of reduction peak current ($I_p^{\rm red}$), peak-to-peak separation (ΔE_p), k^0 , and A_e are presented in Table 1. Through this, alongside Fig. 3C, which provides a comparison of the CVs ($\nu=50~{\rm mV~s^{-1}}$) for each electrode we can see there is no significant variation between the samples, with SWP10–20 showing no underperformance when compared to SWP10–0.

As the majority of analytes are not near-ideal outer sphere probes, the electrodes were tested against the commonly used inner sphere probe $[Fe(CN)_6]^{4-/3}$ (1 mM in 0.1 M KCl). This probe is used regularly throughout the literature on additive manufacturing electrodes, and importantly can give information about the surface accessibility of the conductive components of the electrode, without being affected by oxides or requiring adsorption [61]. Fig. 3D shows the cyclic voltammograms ($\nu = 50 \text{ mV s}^{-1}$) in this case. It can now be seen that upon increasing the amount of biochar embedded within the filament that there is significant decrease in the electrochemical performance of the electrodes once the biochar content is increased above SWP10-2.5. This is also seen when using electrochemical impedance spectroscopy (EIS), Figs. 3E and 3F, where the Nyquist plots show an increasing charge-transfer resistance (R_{CT}), and an increasing solution resistance (R_S), confirmed within Table 1. This data provides additional evidence toward the reduced conductivity of the biochar compared to carbon black, which correlates with the increase in filament resistance seen above. Inclusion of this particular biochar within the filament has a detrimental effect on the conductivity and electrochemical performance of the electrodes but improves the sustainability of it. A compromise

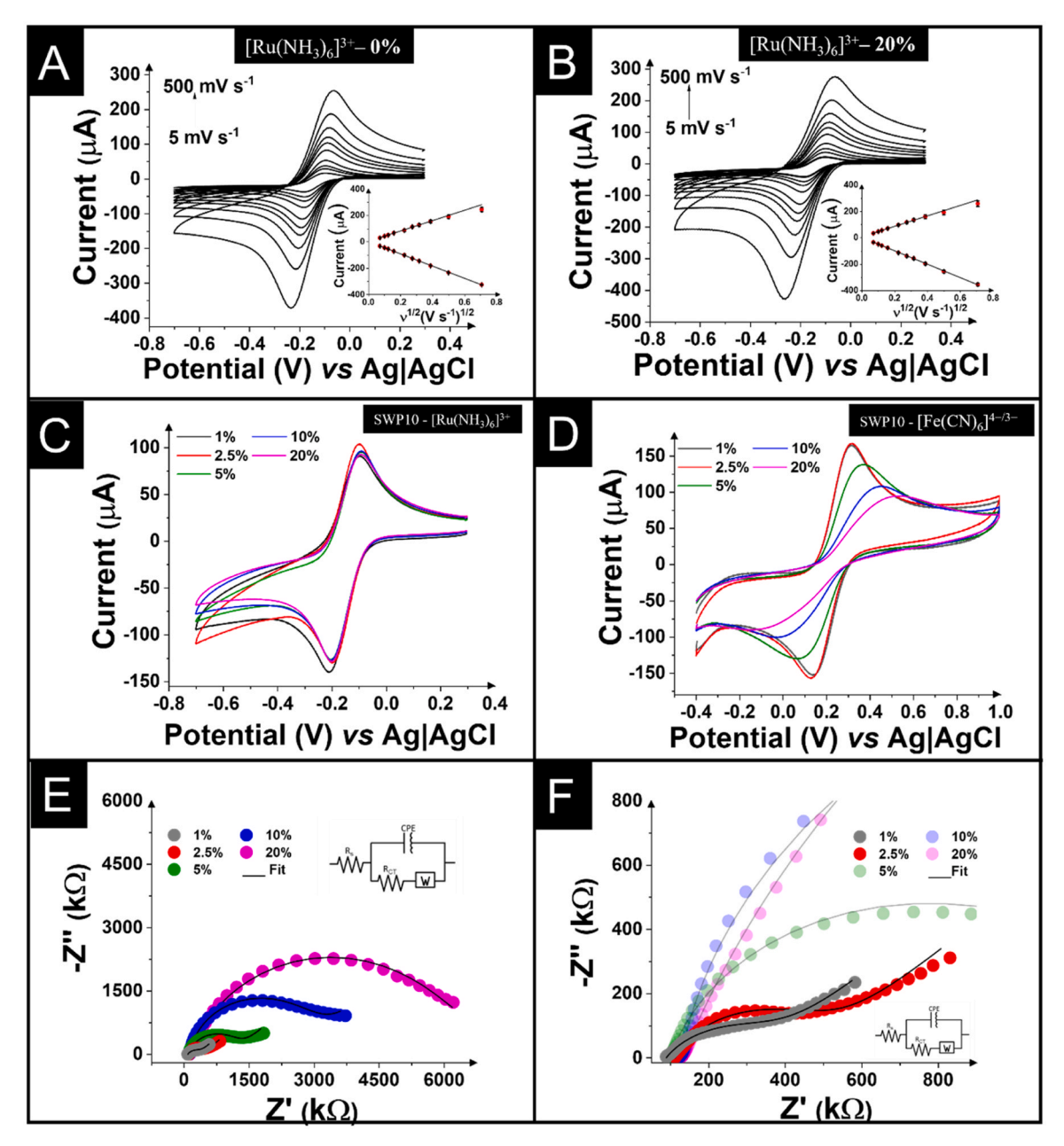


Fig. 3. Scan rate study $(5-500 \text{ mV s}^{-1})$ against $[\text{Ru}(\text{NH}_3)_6]^{3+}$ (1 mM in 0.1 M KCl) performed with the **A**) SWP10–0 electrode and **B**) SWP10–20 electrode. Inset: the Randles–Ševčík plots. Comparison between different percentages of biochar for **C**) $[\text{Ru}(\text{NH}_3)_6]^{3+}$ (1 mM in 0.1 M KCl) and **D**) $[\text{Fe}(\text{CN})_6]^{4-/3-}$ (1 mM in 0.1 M KCl) at scan rate 50 mV s⁻¹. **E**) EIS Nyquist plots in $[\text{Fe}(\text{CN})_6]^{4-/3-}$ comparing different percentages of biochar SWP10. **F**) Enlarged Nyquist plot at higher frequencies and fit for better analysis of the 1 and 2.5 % SWP10 electrodes. Insets: the proposed equivalent circuit.

between these two vital parameters is pursued. We propose that the most sustainable route should be sought whilst meeting the required electrochemical performance for an application.

3.4. Application toward the detection of carbendazim

The objective of this study is not necessarily to develop the highest-performing filament for additive manufacturing electrochemistry but rather to achieve an optimal balance between electrochemical performance and environmental sustainability. From the electrochemical characterisation outlined in the Section 3.3, SWP10–2.5 was clearly the maximum biochar loading available without significantly compromising the voltammetry of inner sphere probes, whereas previously we have established that SWP10–20 is the maximum biochar compatible with a printable filament. As such, for the performance of the electroanalytical

application we choose to consider both cases by applying SWP10–2.5 and SWP10–20 toward the detection of carbendazim (BCM). BCM is a broad-spectrum fungicide that is used within agriculture, horticulture, forestry, and post-harvest food storage and transportation; however, it is regulated in many countries to ensure that the potential health risks of high doses are not realised [49]. Electrodes printed from SWP10–2.5 and SWP10–20 were applied to the detection of BCM within 0.12 M Britton-Robinson (BR) buffer at pH 4 in the concentration range of 0.2–40 μ M. The differential pulse voltammograms (DPV) obtained are presented in Figs. 4A and 4B.

In both cases, voltammograms were obtained with a well-defined peak at $+0.9\,\mathrm{V}$, corresponding to the oxidation of BCM [49]. The associated calibration plots for these are shown within Fig. 4C and D, respectively, where in both cases good linearity is obtained across the whole range. From observing the equations from the lines of best fit,

Table 1 Summary of the electrochemical characteristics calculated through the scan rate studies and electrochemical impedance spectroscopy.

		0 %	1 %	2.5 %	5 %	10 %	20 %
[Ru(NH ₃) ₆] ³⁺	I ^{red} _p (μA) ^a	-71 ± 1	-77 ± 5	-73 ± 7	-74 ± 7	-72 ± 2	-77 ± 4
	$\Delta \mathbf{E_p}^{\mathbf{a}}$	86 ± 4	93 ± 2	80 ± 1	88 ± 4	89 ± 5	91 ± 6
	$A_e (\text{cm}^2)^c$	0.56 ± 0.02	0.61 ± 0.05	0.58 ± 0.05	0.58 ± 0.05	0.56 ± 0.01	0.61 ± 0.02
	$k^0 (x \ 10^{-3} \text{cm s}^{-1})^c$	2.47 ± 0.17	2.13 ± 0.07	2.46 ± 0.15	2.89 ± 1.18	2.27 ± 1.46	2.21 ± 0.26
[Fe(CN) ₆] ^{4-/3-}	$\Delta E_{\mathbf{p}}^{\mathbf{b}}$	137 ± 2	151 ± 12	152 ± 6	231 ± 37	400 ± 63	541 ± 77
	$A_e (cm^2)^d$	0.88 ± 0.07	0.75 ± 0.03	$\textbf{0.84} \pm \textbf{0.03}$	0.47 ± 0.14	0.27 ± 0.04	0.18 ± 0.04
	$k^0 (x 10^{-4} \text{ cm s}^{-1})^d$	9.92 ± 0.32	$\textbf{8.34} \pm \textbf{1.46}$	$\textbf{8.04} \pm \textbf{0.84}$	3.22 ± 1.12	0.71 ± 0.32	0.22 ± 0.14
	$R_S(\Omega)^e$	111 ± 1	89 ± 1	113 ± 1	99 ± 1	127 ± 1	131 ± 1
	$R_{CT} (k\Omega)^e$	443 ± 3	325 ± 3	408 ± 2	1181 ± 2	2900 ± 2	6340 ± 2

All measurements were performed with a nichrome wire CE and Ag|AgCl (3 M KCl) RE.

^e Extracted from Nyquist plots of EIS experiments in [Fe(CN)₆]^{4-/3-} (1 mM in 0.1 M KCl).

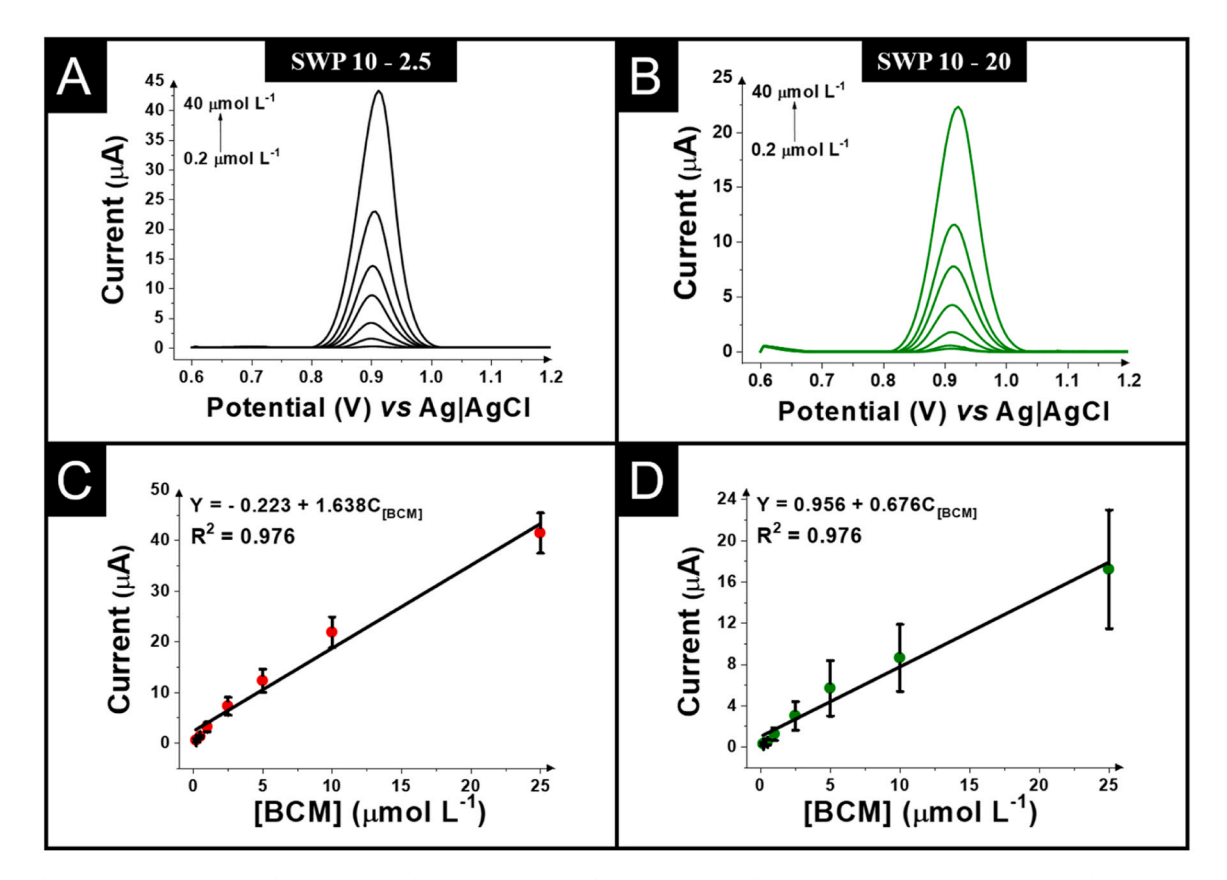


Fig. 4. DP voltammograms for BCM oxidation performed A) SWP10 - 2.5 and B) SWP10 - 20 electrodes in 0.12 M BR buffer pH 4 in the concentration range of 0.2-40 µmol L⁻¹. Calibration plot for the oxidation peak of BCM C) SWP10 - 2.5 and D) SWP10 - 20 electrodes. Step potential: 5 mV. Amplitude: 80 mV.

y = -0.223 + 1.638[BCM] for SWP10-2.5 y = 0.956 + 0.676 [BCM] for SWP10-20, it can be seen that a significant improvement in sensitivity is achieved when using the SWP10-2.5 electrodes. Also, lower values of the standard deviation of each concentration within the calibration curve are observed for the SWP10–2.5. This supports the findings from the previous section where the electrochemical performance against molecules that use an inner sphere mechanism was reduced with increased amounts of biochar. For these electrodes, the detection limit (LOD) and quantification limit (LOQ) were estimated from the equations $LOD = 3sd_B/S$ and $LOQ = 10sd_B/S$, where S is the slope of the analytical curve and sd_B is the standard deviation of the blank response estimated from the average deviation of three blank measurements ($sd_B = 31.04$ nA, for the SWP10-2.5; $sd_B =$ 17.74 nA, for the SWP10-20). The values obtained for the SWP10-2.5

were 0.057 µmol L-1 and 0.19 µmol L-1 for the LOD and LOQ, respectively, while for the SWP10-20, the values were 0.078 µmol L⁻¹ and 0.26 μmol L⁻¹ for the LOD and LOQ, respectively. The results obtained with the proposed electrodes were compared with other studies in the literature on BCM detection in water samples using different electrodes, as presented in Table S1 [62-65]. It was observed that, among the analysed works, the method presented here demonstrated better detectability, as evidenced by a lower LOD and wide linear range when compared to the results reported in the consulted studies.

Finally, both SWP10-2.5 and SWP10-20 electrodes were applied to detect the presence of carbendazim within real spiked river and lake water samples, with the results summarised in Table 2.

From inspection of Table 2, it can be seen that both electrodes achieved excellent recovery values, indicating their applicability for

 $[^]a$ Extracted from 25 mV s $^{-1}$ cyclic voltammogram of [Ru(NH₃)₆] $^{3+}$ (1 mM in 0.1 M KCl). b Extracted from 25 mV s $^{-1}$ cyclic voltammogram of [Fe(CN)₆] $^{4-/3-}$ (1 mM in 0.1 M KCl).

 $[^]c$ Calculated using $\left[Ru(NH_3)_6\right]^{3+}$ cyclic voltammetric scan rate study performed between 5 and 500 mV s $^{-1}$. d Calculated using $\left[Fe(CN)_6\right]^{4-/3-}$ cyclic voltammetric scan rate study performed between 5 and 500 mV s $^{-1}$.

Table 2Summary of the recoveries obtained for the detection of BCM in spiked river and lake water using both the SWP10-2.5 and SWP10-20 additive manufactured electrodes.

Sample	Electrode	Spiked Amount (µM)	Recovery (%)
River Water	SWP10-2.5	25	107.2
	SWP10-20	25	92.5
Lake Water	SWP10-2.5	25	103.9
	SWP10-20	25	100.7

environmental analysis. It is important to note further improvements in sustainability can be made in the future through the use of alternative base polymers, as ingress into PLA hinders the re-use of these electrodes without contamination risk [66]. This work shows as proof-of-concept that biochar can be used to reduce the amount of petrochemically derived conductive carbon within conductive additive manufacturing filament without leading to a detrimental performance. Even when replacing larger amounts of carbon black, the performance can still be more than sufficient to achieve the electroanalytical response required for specific applications. This work shows how, by evaluating the specific needs of the end product, the sustainability of the materials used to produce sensors can be improved. Thinking in this way will allow synergy between the rapid development of electroanalytical platforms and the UN's sustainable development goals.

4. Conclusions

In this work, we report the development of the first conductive additive manufacturing filament using biochar as a conductive filler. The biochar, produced from pyrolysis of softwood pellets, was incorporated into a filament comprised of recycled PLA as the base polymer, carbon black as a supplementary conductive filler and castor oil as a bio-based plasticiser. Two softwood pellet biochars were investigated, SWP and SWP with 10 % ochre added (SWP10). It was found that larger amounts of SWP10 were able to be incorporated into the filament compared with SWP and with SWP10 capable of replacing 20 % of the carbon black whilst still offering good printability. This filament SWP10-20 was physicochemically characterised against SWP10-0 as a benchmark to establish the electrode properties before being electrochemically characterised. Through electrochemical studies of a range of filaments, it was found that SWP10-2.5 produced the best electrochemical performance, whilst SWP10-20 exhibited the least favourable performance toward inner sphere probes. Even so, both these filaments were tested toward the electroanalytical detection of carbendazim, with both electrodes producing excellent result with real-word relevance. The SWP10-2.5 produced a higher sensitivity and lower LOD and LOQ compared to the SWP10-20: however this still performed well when compared to other reported electrodes in the literature. Both biochar-based electrodes were successfully applied to the detection of carbendazim in spiked real river and lake water samples, achieving recoveries between 92.5 – 107.2 %. Through replacing increased amounts of petrochemically derived carbon black with biochar and observing the impact this had on the conductivity, printability, and electrochemical performance of the filaments, we were able to produce filaments with the best compromise between sustainability and performance. This work shows how thinking about the desired end product can allow synergy between the rapid development of electroanalytical platforms and the UN's sustainable development goals.

CRediT authorship contribution statement

Milo Fougerol: Investigation, Formal analysis. Ana Oliveira: Methodology, Investigation, Formal analysis. Karen Augusto: Methodology, Investigation, Formal analysis. Christian Wurzer: Methodology, Investigation, Formal analysis. Muhzamil Khan: Methodology,

Investigation, Formal analysis. Pankaj Singla: Methodology, Investigation, Formal analysis. Ondrej Masek: Methodology, Investigation, Formal analysis. Anjali Jayakumar: Methodology, Investigation, Formal analysis. Marloes Peeters: Writing - review & editing, Writing original draft. Robert Crapnell: Writing - review & editing, Writing original draft, Visualization, Validation, Supervision, Software, Resources, Project administration, Methodology, Investigation, Formal analysis, Data curation, Conceptualization. Craig Banks: Writing - review & editing, Writing - original draft, Visualization, Validation, Supervision, Software, Resources, Project administration, Methodology, Investigation, Funding acquisition, Formal analysis, Data curation, Conceptualization. Elena Bernalte: Writing – review & editing, Writing – original draft, Visualization, Validation, Supervision, Software, Project administration, Methodology, Formal analysis, Data curation, Conceptualization. Rodrigo Muñoz: Writing - review & editing, Writing original draft, Supervision.

Declaration of Competing Interest

The authors declare that they have no known competing financial interests or personal relationships that could have appeared to influence the work reported in this paper.

Acknowledgements

The authors would like to thank Dr Yibing Zhu and Dr Hayley Andrews for the acquisition of SEM and Raman data, respectively. We thank EPSRC for funding (EP/W033224/1), Horizon Europe grant 101137990, the Brazilian agencies: CNPq (402261/2022–4, 315838/2021–3, and 200405/2023–3); CAPES (Project SCBA 88887.658022/2021–00 and 88887.703223/2022–00, and Financial Code 001) and the FAPEMIG (APQ-02391–22) for the financial support.

Appendix A. Supporting information

Supplementary data associated with this article can be found in the online version at doi:10.1016/j.mtcomm.2025.113287.

Data availability

Data will be made available on request.

References

- [1] U. Nations, The 17 Goals.
- [2] U. Nations, Goal 12 Ensure sustainable consumption and production patterns.
- [3] J. Muth, A. Klunker, C. Völlmecke, Putting 3D printing to good use—additive manufacturing and the sustainable development goals, Front. Sustain. 4 (2023) 1196228.
- [4] A. Romani, M. Levi, V. Rognoli, Sustainable development goals enabled by additive manufacturing: a design perspective. UNIDCOM/IADE International Conference Senses & Sensibility, Springer, 2021, pp. 382–397.
- [5] D. Fico, D. Rizzo, R. Casciaro, C. Esposito Corcione, A review of polymer-based materials for fused filament fabrication (FFF): focus on sustainability and recycled materials, Polymers 14 (2022) 465.
- [6] G. Prasad, H. Arunav, S. Dwight, M.B. Ghosh, A. Jayadev, D.I. Nair, Advancing sustainable practices in additive manufacturing: a comprehensive review on material waste recyclability, Sustainability 16 (2024) 10246.
- [7] N. Cakir Yigit, I. Karagoz, A review of recent advances in bio-based polymer composite filaments for 3D printing, Polym. Plast. Technol. Mater. 62 (2023) 1077–1095.
- [8] A. Haryńska, H. Janik, M. Sienkiewicz, B. Mikolaszek, J. Kucińska-Lipka, PLA-potato thermoplastic starch filament as a sustainable alternative to the conventional PLA filament: processing, characterization, and FFF 3D printing, ACS Sustain. Chem. Eng. 9 (2021) 6923–6938.
- [9] M. Guo, J. Han, Q. Ran, M. Zhao, Y. Liu, G. Zhu, Z. Wang, H. Zhao, Multifunctional integrated electrochemical sensing platform based on mesoporous silica nanoparticles decorated single-wall carbon nanotubes network for sensitive determination of gallic acid, Ceram. Int. 49 (2023) 37549–37560.
- [10] H. Zhao, J. Han, M. Zhao, Z. Hui, Z. Li, S. Komarneni, Ultrasensitive electrochemical detection of gallic acid in beverages based on nitrogen-doped

- multi-walled carbon nanotube networks embellished with cobalt 2-methylimidazole nanoparticles, Food Chem. (2025) 142993.
- [11] H. Zhao, M. Zhao, J. Han, Z. Li, J. Tang, Z. Wang, G. Wang, S. Komarneni, Room-temperature fabrication of zeolitic imidazolate framework-8 nanoparticles combined with graphitized and carbonylated carbon nanotubes networks for the ultrasensitive gallic acid electrochemical detection, Food Chem. 465 (2025) 142019
- [12] M.J. Whittingham, R.D. Crapnell, E.J. Rothwell, N.J. Hurst, C.E. Banks, Additive manufacturing for electrochemical labs: an overview and tutorial note on the production of cells, electrodes and accessories, Talanta Open 4 (2021) 100051.
- [13] M.J. Whittingham, R.D. Crapnell, C.E. Banks, Additively manufactured rotating disk electrodes and experimental setup, Anal. Chem. 94 (2022) 13540–13548.
- [14] A.G.-M. Ferrari, N.J. Hurst, E. Bernalte, R.D. Crapnell, M.J. Whittingham, D. A. Brownson, C.E. Banks, Exploration of defined 2-dimensional working electrode shapes through additive manufacturing, Analyst 147 (2022) 5121–5129.
- [15] E. Bernalte, R.D. Crapnell, O.M. Messai, C.E. Banks, The effect of slicer infill pattern on the electrochemical performance of additively manufactured electrodes, ChemElectroChem (2024) e202300576.
- [16] C. Miller, O. Keattch, R.S. Shergill, B.A. Patel, Evaluating diverse electrode surface patterns of 3D printed carbon thermoplastic electrochemical sensors, Analyst 149 (2024) 1502–1508.
- [17] R.S. Shergill, C.L. Miller, B.A. Patel, Influence of instrument parameters on the electrochemical activity of 3D printed carbon thermoplastic electrodes, Sci. Rep. 13 (2023) 339.
- [18] R.S. Shergill, B.A. Patel, The effects of material extrusion printing speed on the electrochemical activity of carbon black/polylactic acid electrodes, ChemElectroChem 9 (2022) e202200831.
- [19] C. Kalinke, N.V. Neumsteir, G. de Oliveira Aparecido, T.V. de Barros Ferraz, P.L. Dos Santos, B.C. Janegitz, J.A. Bonacin, Comparison of activation processes for 3D printed PLA-graphene electrodes: electrochemical properties and application for sensing of dopamine, Analyst 145 (2020) 1207–1218.
- [20] D.P. Rocha, R.G. Rocha, S.V. Castro, M.A. Trindade, R.A. Munoz, E.M. Richter, L. Angnes, Posttreatment of 3D-printed surfaces for electrochemical applications: a critical review on proposed protocols, Electrochem. Sci. Adv. 2 (2022) e2100136.
- [21] R.S. Shergill, F. Perez, A. Abdalla, B.A. Patel, Comparing electrochemical pretreated 3D printed native and mechanically polished electrode surfaces for analytical sensing, J. Electroanal. Chem. 905 (2022) 115994.
- [22] R.D. Crapnell, A. Garcia-Miranda Ferrari, M.J. Whittingham, E. Sigley, N.J. Hurst, E.M. Keefe, C.E. Banks, Adjusting the connection length of additively manufactured electrodes changes the electrochemical and electroanalytical performance, Sensors 22 (2022) 9521.
- [23] R.D. Crapnell, C. Kalinke, L.R.G. Silva, J.S. Stefano, R.J. Williams, R.A.A. Munoz, J. A. Bonacin, B.C. Janegitz, C.E. Banks, Additive manufacturing electrochemistry: an overview of producing bespoke conductive additive manufacturing filaments, Mater. Today (2023).
- [24] J.R. Camargo, R.D. Crapnell, E. Bernalte, A.J. Cunliffe, J. Redfern, B.C. Janegitz, C. E. Banks, Conductive recycled PETg additive manufacturing filament for sterilisable electroanalytical healthcare sensors, Appl. Mater. Today 39 (2024) 102285.
- [25] R.D. Crapnell, E. Bernalte, E. Sigley, C.E. Banks, Recycled PETg embedded with graphene, multi-walled carbon nanotubes and carbon black for high-performance conductive additive manufacturing feedstock, RSC Adv. 14 (2024) 8108–8115.
- [26] A.C. Oliveira, E. Bernalte, R.D. Crapnell, M.J. Whittingham, R.A. Munoz, C. E. Banks, Advances in additive manufacturing for flexible sensors: bespoke conductive TPU for multianalyte detection in biomedical applications, Appl. Mater. Today 42 (2025) 102597.
- [27] D.L. Ramos, R.D. Crapnell, R. Asra, E. Bernalte, A.C. Oliveira, R.A. Muñoz, E. M. Richter, A.M. Jones, C.E. Banks, Conductive polypropylene additive manufacturing feedstock: application to aqueous electroanalysis and unlocking nonaqueous electrochemistry and electrosynthesis, ACS Appl. Mater. Interfaces 16 (2024) 56006–56018.
- [28] R.D. Crapnell, E. Sigley, R.J. Williams, T. Brine, A. Garcia-Miranda Ferrari, C. Kalinke, B.C. Janegitz, J.A. Bonacin, C.E. Banks, Circular economy electrochemistry: recycling old mixed material additively manufactured sensors into new electroanalytical sensing platforms, ACS Sustain. Chem. Eng. 11 (2023) 9183–9193.
- [29] C. Kalinke, R.D. Crapnell, P.R. de Oliveira, B.C. Janegitz, J.A. Bonacin, C.E. Banks, How to improve sustainability in Fused Filament Fabrication (3D Printing) research? Glob. Chall. 8 (2024) 2300408.
- [30] E. Sigley, C. Kalinke, R.D. Crapnell, M.J. Whittingham, R.J. Williams, E.M. Keefe, B.C. Janegitz, J.A. Bonacin, C.E. Banks, Circular economy electrochemistry: creating additive manufacturing feedstocks for caffeine detection from post-industrial coffee pod waste, ACS Sustain. Chem. Eng. 11 (2023) 2978–2988.
- [31] E. Bernalte, R.D. Crapnell, R.El Azizi, K.K.L. Augusto, C.E. Banks, Gold nanoparticle infused castor oil for the production of high performance conductive additive manufacturing filament, Appl. Mater. Today 42 (2025) 102578.
- [32] D.L.O. Ramos, R.D. Crapnell, R. Asra, E. Bernalte, A.C.M. Oliveira, R.A.A. Muñoz, E.M. Richter, A.M. Jones, C.E. Banks, Conductive Polypropylene Additive Manufacturing Feedstock: Application to Aqueous Electroanalysis and Unlocking Nonaqueous Electrochemistry and Electrosynthesis, ACS Appl. Mater. Interfaces 16 (2024) 56006–56018.
- [33] R.D. Crapnell, I.V. Arantes, M.J. Whittingham, E. Sigley, C. Kalinke, B.C. Janegitz, J.A. Bonacin, T.R. Paixão, C.E. Banks, Utilising bio-based plasticiser castor oil and recycled PLA for the production of conductive additive manufacturing feedstock and detection of bisphenol A, Green. Chem. (2023).

- [34] J.P.C. Silva, R.G. Rocha, G.P. Siqueira, C.F. Nascimento, M.H. Santana, E. Nossol, E.M. Richter, I.S. da Silva, R.A. Muñoz, Bio-based plasticizer Babassu oil for custom-made conductive additive-manufacturing filaments: towards 3D-printed electrodes applied to cocaine detection, Microchim. Acta 192 (2025) 1–12.
- [35] L.R. Silva, L.V. Bertolim, J.S. Stefano, J.A. Bonacin, E.M. Richter, R.A. Munoz, B. C. Janegitz, New route for the production of lab-made composite filaments based on soybean oil, polylactic acid and carbon black nanoparticles, and its application in the additive manufacturing of electrochemical sensors, Electrochim. Acta 513 (2025) 145566.
- [36] I.V. Arantes, R.D. Crapnell, E. Bernalte, M.J. Whittingham, T.R. Paixão, C.E. Banks, Mixed graphite/carbon black recycled PLA conductive additive manufacturing filament for the electrochemical detection of oxalate, Anal. Chem. 95 (2023) 15086–15093.
- [37] K.K. Augusto, R.D. Crapnell, E. Bernalte, S. Zighed, A. Ehamparanathan, J. L. Pimlott, H.G. Andrews, M.J. Whittingham, S.J. Rowley-Neale, O. Fatibello-Filho, Optimised graphite/carbon black loading of recycled PLA for the production of low-cost conductive filament and its application to the detection of β-estradiol in environmental samples, Microchim. Acta 191 (2024) 375.
- [38] G. Ravindiran, S. Rajamanickam, G. Janardhan, G. Hayder, A. Alagumalai, O. Mahian, S.S. Lam, C. Sonne, Production and modifications of biochar to engineered materials and its application for environmental sustainability: A review, Biochar 6 (2024) 62.
- [39] P. Prabakar, K. Mustafa Mert, L. Muruganandam, K. Sivagami, A comprehensive review on biochar for electrochemical energy storage applications: an emerging sustainable technology, Front. Energy Res. 12 (2024) 1448520.
- [40] X. Li, J. Zhang, B. Liu, Z. Su, A critical review on the application and recent developments of post-modified biochar in supercapacitors, J. Clean. Prod. 310 (2021) 127428.
- [41] J. Sun, A. Jayakumar, C.G. Díaz-Maroto, I. Moreno, J. Fermoso, O. Mašek, The role of feedstock and activation process on supercapacitor performance of lignocellulosic biochar, Biomass.. Bioenergy 184 (2024) 107180.
- [42] X. Gu, Y. Wang, C. Lai, J. Qiu, S. Li, Y. Hou, W. Martens, N. Mahmood, S. Zhang, Microporous bamboo biochar for lithium-sulfur batteries, Nano Res. 8 (2015) 129–139
- [43] M.J.B. Nogueira, S. Chauque, V. Sperati, L. Savio, G. Divitini, L. Pasquale, S. Marras, P. Franchi, S. Paciornik, R.P. Zaccaria, Untreated bamboo biochar as anode material for sustainable lithium ion batteries, Biomass.. Bioenergy 193 (2025) 107511.
- [44] P. Salimi, S. Tieuli, S. Taghavi, E. Venezia, S. Fugattini, S. Lauciello, M. Prato, S. Marras, T. Li, M. Signoretto, Sustainable lithium-ion batteries based on metalfree tannery waste biochar, Green. Chem. 24 (2022) 4119–4129.
- [45] A.K. Bhakta, R. Fiorenza, K. Jlassi, Z. Mekhalif, A.M.A. Ali, M.M. Chehimi, The emerging role of biochar in the carbon materials family for hydrogen production, Chem. Eng. Res. Des. 188 (2022) 209–228.
- [46] G. Humagain, K. MacDougal, J. MacInnis, J.M. Lowe, R.H. Coridan, S. MacQuarrie, M. Dasog, Highly efficient, biochar-derived molybdenum carbide hydrogen evolution electrocatalyst, Adv. Energy Mater. 8 (2018) 1801461.
- [47] K. Papadopoulou, P.A. Klonos, A. Kyritsis, O. Mašek, C. Wurzer, K. Tsachouridis, A. D. Anastasiou, D.N. Bikiaris, Synthesis and study of fully biodegradable composites based on poly (butylene succinate) and biochar, Polymers 15 (2023) 1049.
- [48] C. Wurzer, O. Masek, Feedstock doping using iron rich waste increases the pyrolysis gas yield and adsorption performance of magnetic biochar for emerging contaminants, Bioresour. Technol. 321 (2021) 124473.
- [49] R.D. Crapnell, P.S. Adarakatti, C.E. Banks, Electroanalytical overview: the sensing of carbendazim, Anal. Methods 15 (2023) 4811–4826.
- [50] J. Li, X. Zhou, C. Zhang, Y. Zhao, Y. Zhu, J. Zhang, J. Bai, X. Xiao, The effects of carbendazim on acute toxicity, development, and reproduction in Caenorhabditis elegans. J. Food Oual. 2020 (2020) 8853537.
- [51] S. Singh, N. Singh, V. Kumar, S. Datta, A.B. Wani, D. Singh, K. Singh, J. Singh, Toxicity, monitoring and biodegradation of the fungicide carbendazim, Environ. Chem. Lett. 14 (2016) 317–329.
- [52] G. Greczynski, L. Hultman, The same chemical state of carbon gives rise to two peaks in X-ray photoelectron spectroscopy, Sci. Rep. 11 (2021) 1–5.
- [53] E.M. Richter, D.P. Rocha, R.M. Cardoso, E.M. Keefe, C.W. Foster, R.A. Munoz, C. E. Banks, Complete additively manufactured (3D-printed) electrochemical sensing platform, Anal. Chem. 91 (2019) 12844–12851.
- [54] C. Wurzer, P. Oesterle, S. Jansson, O. Mašek, Hydrothermal recycling of carbon absorbents loaded with emerging wastewater contaminants, Environ. Pollut. 316 (2023) 120532.
- [55] R.M. Cardoso, C. Kalinke, R.G. Rocha, P.L. Dos Santos, D.P. Rocha, P.R. Oliveira, B. C. Janegitz, J.A. Bonacin, E.M. Richter, R.A. Munoz, Additive-manufactured (3D-printed) electrochemical sensors: a critical review, Anal. Chim. Acta 1118 (2020)
- [56] R. Blume, D. Rosenthal, J.P. Tessonnier, H. Li, A. Knop-Gericke, R. Schlögl, Characterizing graphitic carbon with X-ray photoelectron spectroscopy: a step-bystep approach, ChemCatChem 7 (2015) 2871–2881.
- [57] T.R. Gengenbach, G.H. Major, M.R. Linford, C.D. Easton, Practical guides for x-ray photoelectron spectroscopy (XPS): Interpreting the carbon 1s spectrum, J. Vac. Sci. Technol. A 39 (2021).
- [58] R.D. Crapnell, C.E. Banks, Perspective: What constitutes a quality paper in electroanalysis? Talanta Open 4 (2021) 100065.
- [59] A. García-Miranda Ferrari, C.W. Foster, P.J. Kelly, D.A. Brownson, C.E. Banks, Determination of the electrochemical area of screen-printed electrochemical sensing platforms, Biosensors 8 (2018) 53.
- [60] R.G. Compton, C.E. Banks, Understanding voltammetry, World Scientific, 2007.

- [61] R.L. McCreery, Advanced carbon electrode materials for molecular electrochemistry, Chem. Rev. 108 (2008) 2646–2687.
- [62] A.M. Ashrafi, J. Đorđević, V. Guzsvany, I. Švancara, T. Trtić-Petrović, M. Purenović, K. Vytřas, Trace determination of carbendazim fungicide using adsorptive stripping voltammetry with a carbon paste electrode containing tricresyl phosphate, Int. J. Electrochem. Sci. 7 (2012) 9717–9731.
- [63] S.S. Jonatas de Oliveira, J.F. Dos Santos, H.S. Granja, W.S. Almeida, T.F. Loeser, L. S. Freitas, M.F. Bergamini, L.H. Marcolino-Junior, E.M. Sussuchi, Simultaneous determination of carbendazim and carbaryl pesticides in water bodies samples using a new voltammetric sensor based on Moringa oleifera biochar, Chemosphere 347 (2024) 140707.
- [64] C. Tian, S. Zhang, H. Wang, C. Chen, Z. Han, M. Chen, Y. Zhu, R. Cui, G. Zhang, Three-dimensional nanoporous copper and reduced graphene oxide composites as enhanced sensing platform for electrochemical detection of carbendazim, J. Electroanal. Chem. 847 (2019) 113243.
- [65] L. Wang, M. Li, B. Li, M. Wang, H. Zhao, F. Zhao, Electrochemical sensor based on laser-induced graphene for carbendazim detection in water, Foods 12 (2023) 2277.
- [66] R.J. Williams, T. Brine, R.D. Crapnell, A.G.-M. Ferrari, C.E. Banks, The effect of water ingress on additively manufactured electrodes, Mater. Adv. 3 (2022) 7632–7639.